Diffractive vector meson production at large momentum transfer

J.R. Forshaw
Rutherford Appleton Laboratory,
Chilton, Didcot OX11 0QX, England.
M.G. Ryskin[1]
St. Petersburg Nuclear Physics Institute
188350, Gatchina, St. Petersburg, Russia.

Abstract

The diffractive process $\gamma p \to V + X$ (where V is a vector meson and X results from the dissociation of the proton) is studied. In particular, we consider the region of large momentum transfer (i.e. $|t| \gg \Lambda^2_{QCD}$) and large centre-of-mass (CM) energy, s. The asymptotic ($s \to \infty, s/|t| \gg 1$) behaviour is derived from the BFKL equation and compared to that which is obtained in the Born approximation (two-gluon exchange). We also calculate the corrections to the Born graphs by iterating the BFKL kernel numerically. Improved convergence of the BFKL series is found by summing the logarithms which occur when an exchanged gluon goes nearly on shell. Importantly, we find evidence that the asymptotic solution to the BFKL equation is inappropriate over most of the HERA range and we provide more realistic predictions for the cross section. The predicted cross section is not too small and can be measured at HERA, up to momentum transfers $|t| \sim 10\text{GeV}^2$.

[1]Work supported in part by the Russian Fund of Fundamental Research (93-02-03145) and by the Volkswagen-Stiftung.

1 Introduction

We consider the diffractive production of vector mesons in γp interactions, where the momentum transfer $-t \gg \Lambda^2_{QCD}$ and the photon can be either real or virtual. The vector meson (V) is produced quasi-elastically while the proton dissociates into a diffracted mass, M (this contribution dominates over the elastic channel at large t). The scattering is mediated by the exchange of a colour singlet object, i.e. the perturbative ('hard') pomeron [1, 2]. The largeness of the momentum transfer is expected to guarantee the dominance of short distance physics and hence the use of perturbative QCD. As we shall show, the reaction can be measured up to $-t \sim 10$ GeV^2 at HERA and so we have the possibility to study the hard pomeron in detail. In particular, there is the prospect to examine the QCD pomeron trajectory away from $t = 0$. Elastic (i.e. without proton dissociation) vector meson production by photons at low momentum transfers has been studied in refs.[3, 4, 5, 6].

We start by considering the amplitude corresponding to Feynman graphs like those of figs.1(a,b). The contributions from the more complicated graphs, such as those in figs.1(c,d), will be discussed in section 4. Thus we can factorise the cross section into a product of the usual parton distribution functions and a quasi-elastic 'hard scattering' cross section:

$$\frac{d\sigma^T(\gamma^* p \to V + X)}{dt dx'} = \left(\frac{81}{16} G(x', t) + \sum_f (q(x', t) \; + \; \bar{q}(x', t)) \right) \frac{d\sigma^T(\gamma^* q \to V q)}{dt} \tag{1}$$

and

$$\frac{d\sigma^T(\gamma^* q \to V q)}{dt} = \left(\frac{\alpha_s C_F}{\pi} \right)^4 \frac{\pi^3}{(N_c^2 - 1)^2} \left| \int d^2k d^2k' f^Q(k, k', y) \right|^2 . \tag{2}$$

Here, and throughout the paper, momentum vectors are transverse momentum two-vectors of positive norm. We follow Mueller and Tang [7] in choosing the normalisation such that if $f^Q(k, k', y)$ is the amplitude for scattering two gluons (transverse momenta k and k') then the cross section of eq.(2) is that for quark-quark elastic scattering. The momentum transfer $-t = Q^2$. The separation in rapidity between the final state parton and meson is $y = \ln(\hat{s}/4\bar{q}^2)$ with $\hat{s} = x's$ (s is the $\gamma^* p$ CM energy). We define $\bar{q}^2 = q_\parallel^2 + Q^2/4$ and $q_\parallel^2 = (Q_\gamma^2 + m_V^2)/4$ ($-Q_\gamma^2$ is the photon virtuality). We

use $-t$ and Q^2 interchangeably throughout the paper but it should not cause confusion.

For vector meson production, the amplitude f^Q is the product of the two-gluon scattering amplitude (see eq.(5)) and the form factor associated with the $\gamma^* V$ vertex:

$$\psi_0^V = \mathcal{C}\left[\frac{1}{2\bar{q}^2} - \frac{1}{2q_\parallel^2 + 2(k - Q/2)^2}\right] \tag{3}$$

where

$$\mathcal{C}^2 = \frac{3\Gamma^V_{e^+e^-} m_V^3}{\alpha_{em}}.$$

This is the result of ref.[5] (which is valid for heavy vector mesons, e.g. J/Ψ and Υ). It is written in terms of the electronic width ($\Gamma^V_{e^+e^-}$) of the meson, so as to cancel a large part of the $O(\alpha_s)$-corrections. As usual, $\alpha_{em} = 1/137$, $C_F = 4/3$ and $C_A = N_c = 3$. Although eq.(1) is written for heavy photon-proton interactions, it is also valid in the photoproduction limit, i.e. $Q_\gamma^2 = 0$. Also, eq.(1) is the component of the cross section corresponding to the scattering of transversely polarised photons only. The longitudinal contribution is obtained using $\sigma_L = (Q_\gamma^2/M_V^2)\sigma_T$ and so it dominates at large enough Q_γ^2. Recall that to get the electroproduction (ep) cross section one has to multiply eq.(1) by the photon flux, i.e.

$$\frac{\alpha_{em}}{\pi}\frac{dx}{x}\frac{dQ_\gamma^2}{Q_\gamma^2}(1 - Y + Y^2/2)$$

where x is Bjorken-x and Y is the photon energy fraction ($= Q_\gamma^2/(4xE_eE_p)$).

For the case of quark-quark elastic scattering, the form factor of eq.(3) is replaced by unity and the asymptotic BFKL behaviour of the cross section has been calculated to be [7]

$$\frac{d\sigma(qq \to qq)}{dt} = (\alpha_s C_F)^4 \frac{\pi^3}{4t^2}\frac{\exp(2\omega_0 y)}{[\frac{7}{2}\alpha_s C_A \zeta(3) y]^3}. \tag{4}$$

Where $\zeta(3) \simeq 1.202$ is the Riemann zeta function and $\omega_0 = \frac{C_A\alpha_s}{\pi}4\ln 2$. In the next section, we calculate the cross section for diffractive vector meson production in the same (asymptotic) limit. We obtain analytic expressions in

the limits $|t| \gg q_{\|}^2$ and $|t| \ll q_{\|}^2$. We compare the results with those obtained in the Born approximation (i.e. the two-gluon exchange model of Low and Nussinov [8]). These asymptotic expressions are only valid for $\alpha_s y \gg 1$, i.e. the rapidity interval should be larger than the inverse QCD coupling. For smaller y, we expect significant deviations from the asymptotic formulae, and in section 3 we look for such deviations. Specifically, we iterate the BFKL kernel numerically, so as to obtain corrections to the Born term and to investigate the convergence of the BFKL series (recall it is an expansion in $\sim \alpha_s y$). We perform our calculations up to and including terms $\sim (\alpha_s y)^3$. We also show how to improve the convergence of the series by performing an all orders summation of the logarithms which are large in the asymmetric configurations where one (or more) of the t-channel gluons is nearly on shell. This resummation allows us to make predictions for the diffractive cross section for larger values of y than if we had used the simplest expansion. Of course, for sufficiently large y, even the resummed series is poorly convergent and a full solution to the BFKL equation is required.

It should be acknowledged that, contrary to the case of elastic hadron-hadron scattering [9], the lowest-order photon-hadron amplitude is not sensitive to Sudakov corrections. It was shown in ref.[10] that the Sudakov logarithms, which arise when internal quarks or gluons go on-shell, do not occur due to the pointlike nature of the photon. In addition, due to the largeness of $\bar{q}^2$, we need not worry about vector meson dominance contributions to the vector meson production vertex. This is the case even in the photoproduction limit of $Q_\gamma^2 = 0$.

In section 4 we return to the diagrams of figs.1(c,d). Such diagrams should be important at large $M^2 (\simeq Q^2(1/x' - 1))$. A summary of our results and predictions for cross sections in the HERA range are presented in the conclusion.

2 High energy asymptotics

The solution for the QCD pomeron amplitude at non-zero momentum transfer was given by Lipatov [2] in terms of the eigenfunctions in the transverse coordinate (ρ) representation, i.e.

$$f^Q(k, k', y) = \frac{1}{(2\pi)^6} \int d\nu \frac{\nu^2}{(\nu^2 + 1/4)^2} \exp\left[\omega(\nu) y\right] I_\nu^{A*}(k', Q) I_\nu^B(k, Q), \qquad (5)$$

where

$$I_\nu^A(k,Q) \;=\; V^A(k,Q)\int d^2\rho_1 d^2\rho_2 \left(\frac{(\rho_1-\rho_2)^2}{\rho_1^2\rho_2^2}\right)^{(1+2i\nu)/2} \mathrm{e}^{[ik\cdot\rho_1+i(Q-k)\cdot\rho_2]}. \quad (6)$$

The co-ordinate vectors of the t-channel gluons are ρ_1 and ρ_2 (they are the vectors conjugate to the transverse momentum vectors k and $k-Q$) and $V(k,Q)$ is the 'impact factor' for the vertex, A. For the coupling to a quark line, one can take an impact factor of unity with the modification of eq.(6) which is appropriate for scattering off coloured particles (this is the prescription of ref.[7] and we shall discuss it in more detail in section 4). Whilst for the γ^*V vertex we take the form factor of eq.(3). The function $\omega(\nu)$ is

$$\omega(\nu) = \frac{2\alpha_s C_A}{\pi}\mathcal{R}\mathrm{e}[\psi(1)-\psi(1/2+i\nu)]$$

with $\psi(z) = (d/dz)\ln\Gamma(z)$ (the derivative of the logarithm of the gamma function).

In the high energy limit $y\to\infty$ and the dominant contribution comes from the saddle point at $\nu=0$. Thus we are interested in the function I_0^A. In the qq case it was calculated in ref.[7]:

$$I_0^q(Q) = \int \frac{d^2k}{(2\pi)^2} I_0^q(k,Q) \;=\; -\frac{4\pi}{Q}. \quad (7)$$

In the γ^*V case, things are a little more complicated. Let us define

$$\begin{aligned} V(\rho) \;&=\; \int \frac{d^2k}{(2\pi)^2}\mathrm{e}^{i(k-Q/2)\cdot\rho}\left[\frac{1}{2\bar{q}^2} - \frac{1}{2q_\parallel^2+2(k-Q/2)^2}\right] \\ &=\; \frac{1}{2\bar{q}^2}\delta^{(2)}(\rho) - \frac{1}{4\pi}K_0(q_\parallel\rho), \end{aligned} \quad (8)$$

$R=(\rho_1+\rho_2)/2,\ \rho=\rho_1-\rho_2$ and K_0 is the McDonald function. Now instead of eq.(7), we have

$$\begin{aligned} I_0^V(Q) \;&=\; \mathcal{C}\int d^2R d^2\rho \frac{|\rho|}{|R+\rho/2||R-\rho/2|}\mathrm{e}^{iQ\cdot R}V(\rho) \\ &=\; -\mathcal{C}\int J_0(QR)\; R\,dR\; \frac{|\rho|}{|R+\rho/2||R-\rho/2|}\frac{K_0(q_\parallel\rho)}{2}d^2\rho \end{aligned} \quad (9)$$

and $J_0(x)$ is the Bessel function of the first kind. The cross section is then given by

$$\frac{d\sigma^T(\gamma^* p \to V + X)}{dt dx'} = \left(\frac{81}{16} G(x',t) + \sum_f (q(x',t) \, + \, \bar{q}(x',t))\right) \frac{d\sigma(qq \to qq)}{dt} \times \left[I_0^V(Q) \left(\frac{4\pi}{Q}\right)^{-1} \right]^2, \tag{10}$$

where the quark-quark scattering cross section is given in eq.(4). Eq.(9) can be evaluated analytically[2] in the limits $Q^2 \gg q_\parallel^2$ and $Q^2 \ll q_\parallel^2$.

For $Q^2 \gg q_\parallel^2$ (see ref.[11])

$$I_0^V(Q)|_{Q^2 \gg q_\parallel^2} \simeq -\frac{\mathcal{C}}{Q^3} \ln\left(\frac{4Q^2}{q_\parallel^2}\right) \frac{32\pi^3}{\Gamma^4(1/4)}. \tag{11}$$

In the other limit of small $Q^2 \ll q_\parallel^2$, the essential contribution comes from $R \gg \rho/2$. The logarithmic integral over R goes from $\rho/2$ to $1/Q$ and is equal to $\int_{\rho/2}^{1/Q} \frac{dR}{R} \simeq \ln \frac{2q_\parallel}{Q}$, while the integral $\int_0^\infty d^2\rho\rho \; K_0(\rho q_\parallel) = \pi^2/q_\parallel^3$. So

$$I_0^V(Q)|_{Q^2 \ll q_\parallel^2} \simeq -\frac{\mathcal{C}}{4q_\parallel^3} \ln\left(\frac{4q_\parallel^2}{Q^2}\right) \pi^2. \tag{12}$$

In fig.(2), the results of an exact numerical computation of I_0^V (eq.(9)) are compared with the asymptotic formulae of eqs.(11) and (12), as a function of the ratio $\tau \equiv Q^2/4q_\parallel^2$. This is a sensible variable to plot all our results against, since it exploits the corresponding scale invariance of the BFKL kernel.

To finish the section let us compare the asymptotic BFKL behaviour for the QCD pomeron amplitude with that obtained in the Born approximation. For the two-gluon pomeron the cross section for $\gamma^* q \to Vq$ takes the form

$$\frac{d\sigma^T(\gamma^* q \to Vq)}{dt} = \mathcal{C}^2 \frac{4\pi\alpha_s^4}{81} \mathcal{J}^2, \tag{13}$$

[2]We are indebted to Hans Lotter for correcting a mistake in our initial evaluation of eq.(11)

where

$$\begin{aligned}\mathcal{J} &= \frac{1}{\pi}\int \frac{d^2k}{k^2(Q-k)^2}\left[\frac{1}{2\bar{q}^2} - \frac{1}{2q_\parallel^2 + 2(k-Q/2)^2}\right] \\ &= \frac{8}{Q^4 - 16q_\parallel^4}\ln\frac{(Q^2+4q_\parallel^2)^2}{16Q^2q_\parallel^2}. \end{aligned} \tag{14}$$

For large $Q^2 \gg q_\parallel^2$ the leading logarithmic contribution to $\mathcal{J}$ comes from $q_\parallel^2 \ll (k-Q/2)^2 \ll Q^2/4$ and $\mathcal{J} = \frac{8}{Q^4}\ln\frac{Q^2}{16q_\parallel^2}$. The same logarithmic behaviour arises in the asymptotic BFKL calculation (eq.(11)), which contains an additional enhancement due to the factor $\sim \exp(2\omega_0 y)/y^3$. Note that at not too large energies, the numerical coefficient of the BFKL asymptotic result can be small and for $\omega_0 y \approx 1.5$ it is only about 3% of the Born term.

For small $Q^2 \ll q_\parallel^2$ the BFKL factor of

$$\frac{\pi^4}{4Q^2}\ln^2\frac{4q_\parallel^2}{Q^2}\exp(2\omega_0 y)/[\frac{7}{2}\alpha_s C_A\zeta(3)y]^3$$

is to be compared with the

$$\frac{1}{q_\parallel^2}\ln^2\frac{q_\parallel^2}{Q^2}$$

obtained in the Born approximation. There is an additional enhancement of $\sim q_\parallel^2/Q^2$ in the case of the BFKL pomeron. The origin of the difference is clear. The distance between two gluons in the Low-Nussinov pomeron is fixed since they must couple to the $q\bar{q}$ pair, i.e. their size does not exceed that of the upper vertex ($\rho \sim 1/q_\parallel$). Thus the two-gluon system is not sensitive to small Q^2. However, in the BFKL pomeron, after a few iterations (or rungs of the ladder) the gluons can be separated by large distances $\rho \sim 1/Q$ and so the amplitude $\sim 1/Q$.

3 Iterations of BFKL kernel

So far, we have considered only the asymptotic solution to the BFKL equation. In this section we consider order-by-order iteration of the BFKL kernel for non-zero t and examine the nature of the leading log s expansion. For

sufficiently small z ($= yC_A\alpha_s/2\pi$) (and sufficiently large $|t|$) we can expect the Born approximation to be appropriate. As z increases, so the need to include more and more terms in the BFKL series increases until the point is reached where an all orders summation is vital. By studying the BFKL series in this way we can hope to improve on the Born cross section estimate in the region of intermediate z. In addition, such an expansion will allow us to identify the onset of the region where the BFKL (all orders) resummation is vital. To start, let us recall the BFKL equation for non-zero t:

$$\begin{aligned}\Phi_i(k_i, z_i) = \quad & \frac{1}{\pi}\int_0^{z_i} dz_{i-1} \int \frac{d^2k_{i-1}}{(k_i - k_{i-1})^2} \times \\ & \left\{ \Phi_{i-1}(k_{i-1}, z_{i-1}) \left[\frac{\hat{k}_i^2}{\hat{k}_{i-1}^2} + \frac{k_i^2}{k_{i-1}^2} - Q^2 \frac{(k_i - k_{i-1})^2}{k_{i-1}^2 \hat{k}_{i-1}^2} \right] \right. \\ & \left. - \Phi_{i-1}(k_i, z_{i-1}) \left[\frac{k_i^2}{k_{i-1}^2 + (k_i - k_{i-1})^2} + \frac{\hat{k}_i^2}{\hat{k}_{i-1}^2 + (k_i - k_{i-1})^2} \right] \right\}\end{aligned} \tag{15}$$

For iterations from the quark line we use the boundary condition:

$$\Phi_0(k, z) = 1. \tag{16}$$

As usual, all the k_i are two-vectors in the transverse plane and $\hat{k} = k - Q$. The first iteration of this input leads to the simple expression:

$$\Phi_1(k, z) = z \ln\left(\frac{k^2\hat{k}^2}{Q^4}\right). \tag{17}$$

Subsequent iterations are difficult to perform analytically and we evaluate them numerically.

Successive iterations lead to large oscillatory behaviour in the regions $k^2 \ll Q^2$ and $\hat{k}^2 \ll Q^2$ (as a result of logarithms like the one in eq.(17)). This behaviour leads to a very poorly convergent series. To overcome this difficulty we will sum up the (double) logarithmic contributions $\sim [z\ln(k^2/Q^2)]^n$ analytically, and then factorise these badly oscillating terms to leave behind a better convergent series.

There are no infrared divergences in eq.(15) (neither at $k' \to k$, nor at $k' \to 0$ or $k' \to Q$) and the only logarithm comes from the last (reggeization)

term in the region $k^2 \ll k'^2 \ll Q^2$. For small $k^2 \ll Q^2$ (or $\hat{k}^2 \ll Q^2$) eq.(15) leads to

$$\frac{\partial \Phi(k,z)}{\partial z} = \frac{1}{\pi}\int \frac{d^2k'}{(k'-k)^2}\left\{\left[-\frac{(k'-k)^2}{k'^2}+1+\frac{k^2}{k'^2}\right]\Phi(k',z) - \Phi(k,z)\left[\frac{k^2}{k'^2+(k'-k)^2}+1\right]\right\}, \tag{18}$$

and we have introduced the function $\Phi(k,z)$, where

$$\Phi(k,z) = \sum_{n=0}^{n=\infty}\Phi_n(k,z).$$

We have used the result that $\frac{\partial \Phi_0(k,z)}{\partial z} = 0$. After the angular integration

$$\frac{\partial \Phi(k,z)}{\partial z} = \int dk'^2\left\{\left[-\frac{1}{k'^2}+\frac{1}{|k'^2-k^2|}\left(1+\frac{k^2}{k'^2}\right)\right]\Phi(k',z) - \Phi(k,z)\left[\frac{1+k^2/k'^2}{|k'^2-k^2|}-\frac{k^2/k'^2}{\sqrt{4k'^4+k^4}}\right]\right\}. \tag{19}$$

Which can be written more concisely:

$$\frac{\partial \Phi(k,z)}{\partial z} = \int \frac{d\xi'}{\xi'}\left\{\left[\frac{\xi+\xi'}{|\xi-\xi'|}-1\right](\Phi(k',z)-\Phi(k,z)) + \Phi(k,z)\left[\frac{1}{\sqrt{\frac{4\xi'^2}{\xi^2}+1}}-1\right]\right\}, \tag{20}$$

where $\xi = k^2/Q^2$ and $\xi' = k'^2/Q^2$. It is easy to see that the only logarithmically large contribution comes from the last term, which gives[3] $\Phi(k,z)\ln\xi$ and so

$$\frac{\partial \Phi(k,z)}{\partial z} = 2\left[\int_0^{\xi}\frac{d\xi'(\Phi(k',z)-\Phi(k,z))}{\xi-\xi'}\right.$$

[3]At first sight the accuracy of eq.(18) is insufficient to be sure we are not missing some constant in comparison with the $\ln\xi$. However this log comes only from the reggeization part of the BFKL kernel, for which the exact answer is known. The contribution is equal to $\Phi(k,z)[\ln(Q^2/\mu^2)+\ln(k^2/\mu^2)]$. The infrared cutoff μ^2 is cancelled after we subtract the part

$$2\Phi(k,z)\left[\int_0^{\xi}\frac{d\xi'}{\xi-\xi'}+\int_{\xi}^{\infty}\frac{d\xi'\xi}{\xi'(\xi'-\xi)}\right] = 2\Phi(k,z)\ln(k^2/\mu^2),$$

which has already been included in the integral of eq.(21). Finally one gets $\Phi(k,z)\ln\xi$ and the accuracy of eq.(20) is of the order of $O(k^2/Q^2)$.

$$+ \int_{\xi}^{\infty} \frac{d\xi'(\Phi(k',z) - \Phi(k,z))\xi}{\xi'(\xi'-\xi)} \Bigg] + \Phi(k,z)\ln\xi. \tag{21}$$

In the double log approximation the solution is

$$\Phi(k,z) = \exp\left(z\ln\xi\right)$$

(the integral over ξ' does not give rise to any logs). Now we can put $\Phi(k,z) = \phi(z,\xi)\exp\left(z\ln\xi\right)$ and compute the solution for ϕ

$$\frac{\partial\phi(z,\xi)}{\partial z} = 2\left[\int_0^{\xi} \frac{d\xi'(\phi(z,\xi')(\xi'/\xi)^z - \phi(z,\xi))}{\xi-\xi'}\right.$$

$$\left. + \int_{\xi}^{\infty} \frac{d\xi'(\phi(z,\xi')(\xi'/\xi)^z - \phi(z,\xi))\xi}{\xi'(\xi'-\xi)}\right], \tag{22}$$

with the initial condition $\phi(0,\xi) = 1$ (corresponding to iterations from the quark line). However one can only make sense of such a framework for $z \lesssim 1$. At larger z the last integral in eq.(22) diverges in the region of $\xi' \to \infty$. The implication is that, for $z \gtrsim 1$, eqs.(18-22) are not self-consistent, i.e. the main contribution to $\Phi(k,z)$ (with small ξ) comes from the region of large ξ'. The results of the numerical calculation are presented in fig.3. For $z \lesssim 0.4$ the variations of the function ϕ (from unity) are rather small.

Let us explain how the diffractive cross section is obtained from the $\Phi_m(k,z)$ functions. First define (and we now make explicit the dependence upon the scaling variable $\tau = Q^2/4q_{||}^2$)

$$\psi(z,\tau) = \sum_{n=0}^{n=\infty} \int \frac{d^2k}{\pi} \frac{\psi_m^q(k)\psi_{n-m}^V(k)}{k^2\hat{k}^2} \frac{z^n}{n!} \tag{23}$$

where $\psi_m^q(k)z^m/m! = \Phi_m(k,z)$ is a dimensionless function corresponding to m iterations of the BFKL kernel starting from the quark line boundary condition, $\psi_0^q(k) = 1$. Iterations from the vector meson boundary condition of eq.(3) lead to the functions $\psi_n^V(k)$. The Born term is just the lowest order convolution of eq.(14). The Born term and first iteration from the quark line are known analytically, and the second iteration has been computed numerically. Similarly, the zeroth iteration from the vector meson boundary condition is known analytically, whilst the first iteration can be computed numerically etc.. Consequently, we can convolute these results to obtain

corrections to the Born contribution. Where possible we have checked our results by calculating the convolutions of eq.(23) in different ways, i.e. we have checked that $\psi_1^q \otimes \psi_1^V = \psi_2^q \otimes \psi_0^V$. For the cross section we have

$$\frac{d\sigma^T(\gamma^* q \to Vq)}{dt} = \frac{4\pi\alpha_s^4}{81}|\psi(z,\tau)|^2. \tag{24}$$

After summing the double logarithms

$$\sum_{n=0}^{\infty} \psi_n^q(k)\frac{z^n}{n!} = \exp(z\ln\xi\hat{\xi})\sum_{n=0}^{\infty}\phi_n^q(k)\frac{z^n}{n!}$$

and the equality means that

$$\phi_n^q(k) = \psi_n^q(k) - \psi_{n-1}^q \ln\xi\hat{\xi}\frac{n!}{(n-1)!} + \ldots\ldots + \psi_{n-m}^q(k)\ln^m\xi\hat{\xi}\frac{(-1)^m n!}{(n-m)!m!} + \ldots\ldots$$

We choose to resum terms $\sim z\ln\xi\hat{\xi}$ (this expression simultaneously reduces to the double log solution when $\xi \ll 1$ or $\hat{\xi} \ll 1$). By convoluting the ϕ_n^q functions (rather than the ψ_n^q) with ψ_0^V, in eq.(23), we can compute the double log improved cross section. It should be appreciated that it is only meaningful to perform the exponentiation in the small $\xi\hat{\xi}$ region. Since the integrals (in the convolutions) are performed over all ξ (up to infinity), we must introduce a 'factorisation' scale, ξ_0, to delineate the small $\xi\hat{\xi}$ region, i.e. $\xi\hat{\xi} \leq \xi_0$ must be satisfied before resumming. Choosing $\xi_0 = 0$ therefore corresponds to the un-resummed series. We choose $\xi_0 = 1$ but the choice is essentially arbitrary (in the same way that the QCD factorisation scale is arbitrary). Essentially, the larger one chooses ξ_0, the better the effect of resummation – up to the point where the logarithm of ξ_0 can no longer be considered 'large'.

In figures 4 to 6 we show the dependence of the function $\psi(z,\tau)$ upon τ for different values of z (in fact we plot $[\psi(z,\tau)t^2/(2\mathcal{C})]^2$). These are essentially plots of the cross section, which can be obtained from the plots via eq.(24) and eq.(1). Notice that we have removed the explicit $1/t^4$ behaviour of the cross section to leave behind a quantity which only depends upon the 'scaling' variable, τ, and the 'energy' variable, z. In all cases, the dotted lines are the Born[4] results, the dashed lines include the 1st ($\sim z$) BFKL corrections (to

[4]Or the Born plus the double logs in the case of fig.(5,6).

the Born results), the solid lines include the 2nd ($\sim z^2$) BFKL corrections and the diamonds include the 3rd ($\sim z^3$) BFKL corrections. The dash-dotted lines are obtained using the asymptotic results of the previous section (i.e. the numerical evaluation of eq.(9)). In fig.(4), we show results for the simplest expansion of the BFKL series, i.e. without the double log resummation. Fig.4(a) shows quite clearly the good convergence that is expected for small enough z ($z = 0.05$). The Born term provides a reasonable description and lies within 30% of the higher order result over most of the τ range. The major deviations arise around the dip near $\tau = 1$ (the cross section is zero here in the Born approximation due to the cancellation between the diagrams corresponding to the two gluons coupling to the same and different quark lines). Going to $z = 0.35$, as we do in fig.4(b), we find very poor convergence for $\tau \gtrsim 1$ (where the 2nd and 3rd iterations often deviate by an order of magnitude). The problem is a result of the oscillatory nature of the solutions to the BFKL equation. The first corrections to the Born term are big and they completely fill in the dip. The next corrections tend to restore the dip, by including large negative contributions in the region of $\tau \gtrsim 1$ which partially cancel the positive contribution of the first corrections. This leads to the unpredictable behaviour of fig.4(b). We do not expect, therefore, to make reliable predictions for the diffractive cross section using such a simple minded expansion of the BFKL series (for all but the smallest values of z). Before moving on to the results obtained with the resummed series we should point out that, as noted above, the poorest convergence of the un-resummed series occurs for the larger values of τ, (in particular in the region around the dip) and that this is a general feature of our results. Indeed we shall see that it is precisely this region that is improved by resumming. This is to be understood as the region where the asymmetric configuration (i.e. where one of the gluons which couples to the γV vertex carries all the momentum transfer) is important.

The double log improved results are shown next. Fig.5 shows the analogous plots to those in fig.4. The accuracy of the (resummed) Born term is improved at $z = 0.05$, whilst at $z = 0.35$ the higher corrections are necessary. However, for $z = 0.35$, we can now claim to make reasonable predictions over the whole τ range after just two iterations of the BFKL kernel, i.e. the difference between the 2nd and 3rd iterations is typically $\lesssim 20\%$. Fig.6 shows the resummed results for $z = 0.2, 0.5$ and 0.8 (which are typical values for HERA). For $z = 0.2$ we obtain convergence at the level of $\sim 1\%$ at order

z^3. Going to larger z, as one expects, the quality of convergence deteriorates and, at $z = 0.8$, we clearly need a more complete summation of the BFKL series. However, it is essential to realise (since the cross section is expected to vary rapidly with the momentum transfer) that a prediction of the cross section to within a factor ~ 2 is very useful. For example, at $z = 0.8$, the Born cross section lies typically more than an order of magnitude (~ 50) below the order z^3 results (diamonds), which is in turn a factor $\sim 2-3$ below the asymptotic results.

Comparison of the numerical results obtained in this section with the asymptotic results (dash-dot lines) shows quite clearly that the asymptotic formulae do not represent the diffractive cross section over most, if not all, of the kinematic range examined. Only at the largest value of z, does it look likely that, after fully summing the BFKL series, the result will agree with the asymptotic prediction. In the region where the double logarithmic resummation is most important, i.e. $\tau \gtrsim 1$, the asymptotic formulae fail completely to approximate even the gross features of the expected shape, e.g. the dip. In addition, the asymptotic prediction always appears to overestimate the size of the cross section. Ultimately, for large enough z, the asymptotic result must be more appropriate than the 'fixed order' results. We can see, in fig.6, that at $z = 0.8$ the BFKL series is slowly convergent and one can no longer trust the order z^3 predictions, i.e. this marks the onset of the dynamics manifest in the full BFKL solution which will ultimately be described by the asymptotic solution. It should not come as a surprise that the asymptotic prediction is not trustworthy for $z \lesssim 1$. Its reliability relies upon the validity of the approximation that the exponential in eq.(5) can be expanded about $\nu = 0$. This is a very poor approximation for $z \lesssim 1$ since the integrand of eq.(5) actually vanishes at $\nu = 0$ and rises rapidly to its maximum value only for large z.

It is also worth commenting upon the results of Lipatov [2] and of Hancock and Ross [12]. They have found that, in the case of a running $\alpha_s(\mathrm{Max}(k^2, Q^2))$, the leading eigenvalue of the BFKL kernel lies somewhat below its asymptotic value for all realistic energies (and non-zero t). Therefore the cross section is expected be smaller than that predicted by the asymptotic solution based on eq.(4). We do not investigate the effect of a running coupling here.

4 Sub-leading Corrections

We have devoted a whole section to the calculation of the process $\gamma^* q \to V q$. We now turn to a discussion of the 'lower part' of the diagram and the validity of the simple assumption that the pomeron couples to a single parton inside the proton.

If Q^2 is large enough, so that the partons (which we label by their longitudinal momentum fractions x' and x'') within the proton are separated by distances $\rho' \gg 1/Q$ then we are certainly entitled to restrict ourselves to the simple coupling to a single parton line. This may seem somewhat suprising, since at first sight eq.(6) appears to suggest that the only contribution arises from the coupling to different parton lines (the amplitude vanishes at $\rho_1 = \rho_2$): This is not the case. To exploit the conformal invariance, Lipatov redefined the eigenfuctions (by adding terms proportional to $\delta^{(2)}(k)$ and $\delta^{(2)}(k-q)$ which vanish on coupling to colourless particles) and so the contribution from the Feynman graphs where the pomeron couples to a single parton is hidden. Indeed, let us start by assuming that $\rho' \gg 1/Q$, such that (for large Q^2)

$$\int d^2R \, \mathrm{e}^{iQ\cdot R} \frac{\rho}{|R+\rho/2||R-\rho/2|} \approx \frac{2\pi}{Q}(\mathrm{e}^{iQ\cdot\rho/2} + \mathrm{e}^{-iQ\cdot\rho/2}), \tag{25}$$

i.e. the main contributions arise from the regions where R is within $\Delta R \sim 1/Q$ of the singular points at $\pm\rho/2$. This is the result which underpins the Mueller-Tang prescription for calculating the contribution from the coupling to a single parton line. The first term of the r.h.s. of eq.(25) corresponds to interaction with a quark at $\rho' = \rho/2$ whilst the second term is due to interaction with an anti-quark at $-\rho/2$. Corrections to eq.(25) are $\sim (\Delta R/\rho)^2 \sim 1/(\rho^2 Q^2)$ and represent contributions from Feynman graphs where the pomeron couples to more than one parton.

Note that this approach is not appropriate for the γV vertex. In evaluating the R integral of eq.(9) we are not entitled to assume that the essential contributions arise from the regions around the singular points since the subsequent ρ integral would be dominated by contributions from small $\rho \sim 1/Q$, i.e. after evaluating the R integral using eq.(25), we would be left with

$$\int K_0(q_{||}\rho)\mathrm{e}^{iQ\cdot\rho/2} d^2\rho$$

where the dominant contribution arises from small $\rho \sim 1/Q$ and thus we are not justified in assuming that $\rho \gg \Delta R$. The corrections are therefore essential and indeed give the main contribution to $I_0^V(Q)$ (i.e. the logarithm in eq.(11)) at large Q^2.

At the lower vertex, the situation is quite different since the target dissociates. The impact factor now takes the form,

$$|I_0^p(Q)|^2 = 2\int d^2\rho\, d^2R\, d^2R'\, |\Psi(\rho)|^2 \frac{\rho\, \mathrm{e}^{iQ\cdot R}}{|R-\rho/2||R+\rho/2|}\frac{\rho\, \mathrm{e}^{-iQ\cdot R'}}{|R'-\rho/2||R'+\rho/2|} \tag{26}$$

where $|\Psi(\rho)|^2$ is analogous to $V(\rho)$ in eq.(8). The integrals over R and R' can now be performed safely in the $\rho \gg \Delta R$ limit since the exponentials ($\mathrm{e}^{iQ\cdot\rho/2}$ and $\mathrm{e}^{-iQ\cdot\rho/2}$) cancel each other. Thus we get

$$|I_0^p(Q)|^2 = \frac{16\pi^2}{Q^2}\int d^2\rho |\Psi(\rho)|^2. \tag{27}$$

With the lower limit of the ρ integral equal to $1/Q$ and the upper limit fixed by the proton radius the integral over Ψ gives the conventional structure function, i.e. $|\Psi|^2 \sim 1/\rho^2$ generates the leading logarithmic behaviour of the parton density function with the typical values of $\rho \gg 1/Q$. Since the integrand of the ρ integral is independent of Q^2 (it is simply the wavefunction) it follows that the main term in eq.(26) is indeed the contribution from the graphs where the pomeron couples to a single parton line. Thus we have obtained the Mueller-Tang result that was used in the first part of the present paper and have justified our assumption that the dominant contribution to the proton dissociation (at large enough Q^2) arises from the coupling to a single parton line. For a more detailed discussion of the nature of the pomeron-quark coupling we refer to ref.[13].

Note that we neglected the cross terms $\sim \mathrm{e}^{iQ\cdot\rho}$ which arise from the points $R \to \pm\rho/2$; $\quad R' \to \pm\rho/2$ after the R and R' integrals of eq.(26). They represent contributions from the interference between graphs where the pomeron couples to single but different parton lines. Such contributions are suppressed at least by logarithms of Q^2 since the momentum transfer must flow into the proton wavefunction.

Similarly, diagrams like the one of fig.1(c) are beyond the leading $\ln Q^2$ approximation since they lose at least one power of $\ln Q^2$ due to the hooking of the large transverse momentum, $k \sim Q/2$ into lower rungs of the 'structure

function'.[5] Therefore the contributions from such graphs are suppressed in comparison with those of figs.1(a,b) by the factor $-\frac{1}{2}\gamma_2$. The anomalous dimension of the twist-2 operator (structure function) is $\gamma_2 \propto \alpha_s$ and its presence reflects the fact that one loses one power of $\ln Q^2$. The additional smallness $(-1/2)$ comes from the colour coefficient ($C_A/2$ in comparison with C_A). Note that the coefficient is negative and so the graph in fig.1(c) describes a colour screening effect. If the BFKL gluon continues down and touches the next s-channel gluon (i.e. x''') then one gets a factor of $1/4$ and two powers of γ_2, and so on. When computing the cross section, one must remember to double the contributions from configurations where the two t-channel gluons couple to different s-channel gluons. Finally, if the two gluons couple to the same s-channel gluon (x'') then one loses one logarithm and picks up a colour coefficient which is the square of the result obtained when the gluons couple to different gluons. Thus the leading contribution to the order α_s corrections is suppressed relative to the contributions of figs.1(a,b) by the factor

$$T_2 \;=\; \left(-\frac{1}{2}-\frac{1}{2}+\frac{1}{4}\right)\gamma_2 = -\frac{3}{4}\gamma_2 \simeq -0.3. \tag{28}$$

We put $\alpha_s = 0.16$ and use the double logarithmic approximation result: $\gamma_2 = C_A\alpha_s/(\pi\omega) \simeq 0.36$ with $\omega = \omega_0 = 0.42$. Such contributions correspond to the $\sim 1/(\rho^2 Q^2)$ corrections to the impact factor, $I_0^p(Q)$, calculated above.

Let us now turn to graphs like the one shown in fig.1(d). Such diagrams differ from those of fig.1(c) in the sense that one of the gluons now couples deep inside the proton (e.g. to a different branch of the parton cascade). As such we expect a power like suppression combined with an enhancement due to the sampling of the two-parton component of the hadron wavefunction. Let us estimate the possible size of such contributions. The contribution is analogous to the graph of fig.1(b), in the sense that the pomeron is coupling to different parton lines in the scattered object. Unlike the case of fig.1(b) however, its contribution is not calculable in perturbation theory since it is dependent upon the rather complicated structure of the proton wavefunction. Since the proton is more diffuse than the compact quark-antiquark pair (of

[5]It was shown in section 2 that for large y the internal momenta inside the BFKL ladder are typically $k \sim Q/2$. The contribution from the region of small k (or $(Q-k)$) dies out with energy. Even in the Born (two-gluon) approximation the main logarithmic contribution comes from $(k - Q/2) \ll Q/2$, i.e. k close to $Q/2$.

the upper vertex) we anticipate that fig.1(d) will be suppressed at all values of the momentum transfer considered here, i.e. $Q \gg \Lambda_{QCD}$.

In comparison with eq.(1), the contribution of the graph of fig.1(d) to the cross section contains an additional colour factor $1/(N_c^2-1) = 1/8$. There is additional suppression from the integration over the transverse momenta of the t-channel gluons, k_1 and $k_2(= Q - k_1)$, which connect the pomeron and the proton. In the case of fig.1(a,b) there were no correlations between the momenta (k_1 , k_2) in the amplitude A and the corresponding momenta (k_1' , k_2') in the complex conjugated amplitude A^*. One therefore has independent integrals over k_1 and k_1' which give two large (of the order of Q^2) factors. This is not the case for the diagram of fig.1(d). The transverse momentum, k_2, is typically carried away by its associated final state gluon which means that $k_2 \sim k_2'$ and we get only one large integral which is $\sim Q^2$. The remaining integral is then over the intrinsic gluon momentum, δk ($k_2' = k_2 + \delta k$) and we become sensitive to non-perturbative effects in the proton, i.e. the momentum transferred over the k_2' loop in fig.1(d) is limited by the wave function of the target nucleon. However, there is an enhancement due to the larger combinatorial factor associated with coupling the two-gluons to different parton lines.

We can be more explicit by returning to the impact parameter representation. As we have just shown, the square of the impact factor for coupling the pomeron to a single parton line is $\propto (4\pi/Q)^2$ (eq.(7,27)) and to obtain the cross section, we then multiplied by the parton density factor (which can be thought of as the multiplicity associated with the pomeron-proton impact factor). An analogous, but slightly more involved, calculation can be performed for the case of the diagrams like that in fig.1(d), i.e. we can compute the square of the impact factor and multiply by the colour factor (1/8) and the square of the parton densities to obtain the cross section. The impact factor can be written thus:

$$\begin{aligned} |\Delta I_0^p(Q)|^2 &= 2\int d^2\rho\, d^2R\, d^2R'\, |\Psi_2(\rho)|^2 \times \\ &\quad \left[\frac{\rho\, \mathrm{e}^{iQ\cdot R}}{|R-\rho/2||R+\rho/2|}\frac{\rho\, \mathrm{e}^{-iQ\cdot R'}}{|R'-\rho/2||R'+\rho/2|} - \mathrm{M.T.}\right]. \end{aligned} \quad (29)$$

The Mueller-Tang subtraction term (denoted by 'M.T.') is defined by the

replacement:

$$\int d^2R \frac{\rho\ \mathrm{e}^{iQ\cdot R}}{|R-\rho/2||R+\rho/2|} \to \int d^2R \frac{\rho\ \mathrm{e}^{iQ\cdot R}}{|R-\rho/2||R+\rho/2|} - \frac{2\pi}{Q}(\mathrm{e}^{iQ\cdot\rho/2}+\mathrm{e}^{iQ\cdot\rho/2})$$

and similarly for the R' integral. In this way we remove the contribution corresponding to the coupling to a single parton line. The answer, as it must be, is sensitive to the large distance physics of the nucleon and this is contained in the two-particle wavefunction $\Psi_2(\rho)$. Dependence upon longitudinal momenta is assumed to factorise into the parton number densities.

We use a gaussian form for the ρ distribution and can introduce the same scale, Q_0^2, that is used by L.V. Gribov, Levin and Ryskin (GLR) to parameterise the screening corrections to the deep inelastic structure functions [14, 15], i.e.

$$|\Psi_2(\rho)|^2 = \frac{Q_0^2}{4\pi}\mathrm{e}^{-\rho^2 Q_0^2/4} \tag{30}$$

with $Q_0^2 = 1.2$ GeV^2 from fits to $Sp\bar{p}S$ data (mainly on the inclusive cross section for charged hadron production).

Eq.(29) can be simplified, i.e.

$$|\Delta I_0^p(Q)|^2 = 2\int d^2\rho\ \rho^2 |\Psi_2(\rho)|^2\ J_x(\rho)J_y(\rho) \tag{31}$$

where

$$\begin{aligned}\frac{J_x(\rho)}{2}\mathrm{e}^{iQ\cdot\rho/2} &= \int_0^{1/2} dx \left\{ \frac{K_0(Q\rho\sqrt{x(1-x)})}{\sqrt{x(1-x)}}(\mathrm{e}^{ixQ\cdot\rho}+\mathrm{e}^{i(1-x)Q\cdot\rho}) \right. \\ &- \left. \frac{K_0(Q\rho\sqrt{x})}{\sqrt{x}}(1+\mathrm{e}^{iQ\cdot\rho}) \right\} \\ &- \int_{1/2}^{\infty} dx \frac{K_0(Q\rho\sqrt{x})}{\sqrt{x}}(1+\mathrm{e}^{iQ\cdot\rho}).\end{aligned} \tag{32}$$

and similarly for $J_y(\rho)$. In the limit $Q/Q_0 \gg 1$ the integral is dominated by the contribution from $x \sim 1/(Q\rho)^2 \ll 1$ and $\rho \sim 1/Q_0$. We can thus neglect the integral over $x > 1/2$. After expanding the exponentials and performing the remaining integrals we obtain:

$$|\Delta I_0^p(Q)|^2 = \frac{16\pi^2}{Q^2}\frac{Q_0^2}{4Q^2}S \tag{33}$$

with $S \sim \ln(Q/Q_0)$. We also computed S numerically, and for $4Q^2/Q_0^2 = 10$ we get $S = 0.74$.

Combining eq.(33) with the colour factor and the square of the parton densities we can now estimate the size of the corrections which originate from fig.1(d), i.e. we have, rather than the factor $G(x', t)dx'$, the term

$$\frac{S}{8}\left(\frac{Q_0^2}{4Q^2}\right) G(x_1, Q^2/4)G(x_2, Q^2/4)dx_1 dx_2. \tag{34}$$

Now let us talk a little more about the value of Q_0. At first sight, one might anticipate that $Q_0 \sim 1/R_N$ (the inverse proton radius). However from the semihard phenomenology of ref.[15] we know that the gluon-gluon correlation length R_0 is much smaller than R_N. Also, calculations based upon QCD sum rules determine the radius of the two-gluon form factor of the proton to be $R_0 \simeq 0.3 - 0.35$ fm [16], which corresponds to $Q_0^2 \simeq 1.2$ GeV^2. We should point out that we have ignored corrections due to interactions between the two branches of the parton cascade (i.e. we used the square of the single parton density in eq.(34)).

We are ready to make a numerical estimate for the size of this correction. The integrations over x_1 and x_2, in eq.(34), are limited by the mass of the hadron system $M^2 \simeq \frac{|t|}{4}\left(\frac{1}{x_1} + \frac{1}{x_2}\right)$ or by other experimental conditions. For example, one might choose to search for jets in the proton dissociation. This would be a useful search to perform, since it would not only give an additional way to measure the momentum transfer (and the momentum fractions x_1 , x_2 carried by the jets) but it could be used as a means to distinguish between the leading and sub-leading contributions (for the sub-leading contribution, the vector meson transverse momentum is balanced by a pair of jets each with transverse momentum $\sim Q/2$, while in the leading case it is balanced by the one jet). Unfortunately, it is not easy to make such a study at HERA since the need to ensure a large rapidity gap forces the jets to lie close to the beam hole. Since we do not require the observation of the proton dissociation, we shall estimate the sub-leading corrections assuming no jets are seen in the proton direction, i.e.

$$\theta \simeq \frac{\sqrt{|t|}/2}{xE_p} < 3^o$$

in HERA lab frame then

$$x_{1,2} > x_m \;=\; \frac{\sqrt{|t|}}{2E_p\theta} \approx 0.02$$

for $|t| = 3$ GeV^2. Thus we find the ratio of the leading to sub-leading contributions to be

$$\begin{aligned} &\approx \frac{\frac{S}{8}\left(\frac{Q_0^2}{4Q^2}\right)\int_{x_m}^1 G(x_1,Q^2/4)dx_1 G(x_2,Q^2/4)dx_2}{\int_{x_m}^1 G(x',t)dx'} \\ &\approx \frac{S}{8}\left(\frac{Q_0^2}{4Q^2}\right)\int_{x_m}^1 G(x,Q^2/4)dx \approx \frac{0.18S\ \text{GeV}^2}{|t|} \end{aligned} \tag{35}$$

and we have put $x_m = 0.02$. Taking $Q^2 = 1.2$ GeV^2 and $|t| \gtrsim 3$ GeV^2 (i.e. $S \approx 0.74$) it follows that this ratio is $\lesssim 5\%$.

As we mentioned above, perhaps the best way to study the sub-leading contributions would be to look at the jet structure of the final state. At high enough centre of mass energies one can have a large diffracted mass and still maintain a rapidity gap. Events with a large diffracted mass will lead to relatively large values for the sub-leading corrections (since x_1 and x_2 can be small).

Based on these estimates we think that, over the HERA range, the sub-leading corrections discussed here do not change the results of the previous calculations (which assume factorisation of the proton dissociation) in a crucial manner. The effect may be less than $\approx 5\%$ for dissociation into a small mass, but it would be interesting to study experimentally how it reveals itself at higher masses.

5 Conclusion

We have studied the hard diffractive production of heavy vector mesons in deep inelastic scattering. The hardness is provided by a large momentum transfer, $|t|$, and allows one to probe the essential dynamics which determine the pomeron of perturbative QCD. We have made predictions for the cross section for a range of kinematical configurations accessible at HERA. Corrections to the simple two-gluon picture of the pomeron have been computed

using the leading logarithmic formalism of BFKL and they are seen to be very large.

It is encouraging that the total cross section for this process is not too small. Specifically, for $\sqrt{s} \approx 200$ GeV, photon virtuality $Q_\gamma^2 \approx 10$ GeV^2, $x' \gtrsim 0.01$ and $|t| \geq 2$ GeV^2 (i.e. a mean z of 0.6) the total cross section $\sigma^T(\gamma^* p \to V + X)$ for the hard diffractive production of J/Ψ mesons is ≈ 1.5 nb. This is to be compared with the asymptotic BFKL prediction of ≈ 3 nb and the Born prediction of ≈ 84 pb. Although this cross section (1.5 nb) is small, (it is only 0.01% of the total DIS cross section) it is not prohibitively so.

Although we have concentrated on the general case of non-zero Q_γ^2, all of our results could equally well apply to photoproduction (where the production rate is much higher). We need not worry about Sudakov or VMD corrections due to the largeness of $\bar{q}^2$. For example, for $Q_\gamma^2 = 0$, $\sqrt{s} = 200$ GeV and $|t| \geq 2$ GeV^2 one is probing a mean z of 0.8 and the cross section for J/Ψ production off transverse photons is ≈ 15 nb. At $\sqrt{s} = 100$ GeV this cross section falls to ≈ 5 nb.

It is an important asset of this process that one does not need to observe the products of the proton dissociation in order to extract the momentum transfer, t. In DIS, observation of the scattered electron together with the decay products of the vector meson allows a clean determination of t whilst in photoproduction one can assume that the incoming photon is collinear with the incoming electron and hence the p_T of the vector meson gives t. Consequently, the rapidity gap between the vector meson and the scattered parton can be as big as 9 units. As a result, HERA can probe the region where the BFKL series is poorly convergent, i.e. where the resummation of leading $\ln s$ terms is most important.

We restricted ourselves to heavy mesons for reasons of simplicity although ρ (or ϕ) production will also provide important information on the QCD pomeron with generally a much higher production rate. Our calculations have been totally general and so one could use them to predict the production cross sections for any vector meson. However, we expect the non-relativistic approximation to be less appropriate for the light mesons. In addition, VMD contributions may well start to become significant in the case of photoproduction for not-too-large t. It is interesting to note that for $|t| \gg m_V^2$ the yield of heavy vector mesons is larger than that of the lighter ones. This

is because the cross section for scattering transversely polarised photons is proportional to $\Gamma^V_{e^+e^-} m_V^3$ (see eqs.(1),(3)). Since the electromagnetic widths of the J/Ψ and ρ are similar we therefore find the J/Ψ rate to be enhanced by a factor ~ 50 over the ρ production rate. This is a simple consequence of the fact that at large $|t|$, the pomeron has enhanced coupling to the more compact $c\bar{c}$ pair which constitutes the J/Ψ. However, this enhancement is diluted to a single power of m_V in the case of longitudinal photon scattering, which dominates at large enough photon virtualities. We note that changing the photon virtuality allows one to scan through the vector meson wave function (as was discussed in ref.[17]).

Corrections to our predictions which arise from higher order QCD and non-perturbative effects (in the dissociation of the proton) have been estimated and should not be essential over the HERA range, perhaps contributing by no more than $\approx 5\%$. However, higher order corrections to the BFKL amplitude itself may be more significant. For example, if we take $y = \ln[\hat{s}/(4\mathrm{Max}(Q_\gamma^2, m_V^2, Q^2))]$ (rather than $y = \ln(\hat{s}/4\bar{q}^2)$) then the cross sections quoted in these conclusions are reduced by $\sim 40\%$. This ambiguity in the definition of y is a direct consequence of the leading log nature of the calculation.

It should not be long before the HERA experiments are able to study data in the regime considered in this paper. In particular, there is already some preliminary data on both J/Ψ and ρ production out to $|t|$ values as large as 1.5 GeV^2 (in DIS and photoproduction) and at γp centre-of-mass energies of ≈ 100 GeV [18].

Acknowledgements: We should like to thank Prof. M.Arneodo, Dr. H.Jung, Prof. C.Peroni and Dr. P.J.Sutton for many fruitful discussions. Very special thanks to Prof. J.Bartels, H.Lotter and Dr. M.Wüsthoff for their interest in this work. One of us (M.R.) gratefully acknowledges the hospitality of the Torino University Physics Department, the Theory Group of the RAL Particle Physics Department and the DESY Theory Division, where part of this work was done.

References

[1] V.S.Fadin, E.A.Kuraev, L.N.Lipatov: Sov.Phys.JETP 45 (1977) 199; Ia.Ia.Balitski, L.N.Lipatov: Sov.J.Nucl.Phys. 28 (1978) 822

[2] L.N.Lipatov: Sov.Phys.JETP 63 (1986) 904

[3] A.Donnachie, P.V.Landshoff: Phys.Lett. B185 (1987) 403

[4] J.R.Cudell: Nucl.Phys. B336 (1990) 1

[5] M.G.Ryskin: Z.Phys. C57 (1993) 89

[6] S.J.Brodsky et al.: Phys.Rev. D50 (1994) 3134

[7] A.H.Mueller, W.K.Tang: Phys.Lett. B284 (1992) 123

[8] F.E.Low: Phys.Rev. D12 (1975) 163; S.Nussinov: Phys.Rev.Lett. 34 (1975) 1286

[9] J.Botts, G.Sterman: Phys.Lett. B224 (1989) 201; Nucl.Phys. B325 (1989) 62

[10] G.R.Farrar, G.Sterman, H.Zhang: Phys.Rev.Lett. 62 (1989) 2229

[11] J.Bartels et al.: in preparation.

[12] R.E.Hancock, D.A.Ross: Nucl.Phys. B394 (1993) 200

[13] J.Bartels et al.: 'How does the BFKL pomeron couple to quarks?', DESY-94-244.

[14] L.V.Gribov, E.M.Levin, M.G.Ryskin: Phys.Rep. 100 (1983) 1

[15] E.M.Levin, M.G.Ryskin: Phys.Rep. 189 (1990) 267

[16] V.M.Braun, R.Gornicki, L.Mankiewicz, A.Schäfer: Phys.Lett. B302 (1993) 291

[17] B.Z.Kopeliovich, J.Nemchick, N.N.Nikolaev, B.G.Zakharov: Phys.Lett. B309 (1993) 179

[18] ZEUS Collab., M.Derrick et al.: 'Observation of vector meson production in electron-proton DIS at HERA', ICHEP94 Ref. 0663; ibid. 'Cross Section Measurement of the process $ep \to epJ/\Psi$ at HERA', ICHEP94 Ref. 0672; I.Abt et al.: H1 Collaboration, 'Photoproduction of J/Ψ Mesons at HERA', DESY 94-153.

Figure Captions

Fig. 1 Feynman graphs corresponding to diffractive vector meson production in DIS.

Fig. 2 The asymptotic prediction for the diffractive scattering amplitude. The dotted lines are the analytical approximations and the solid line is the result of exact numerical computation.

Fig. 3 The deviation of solution of the BFKL equation in the low ξ region from the double logarithmic form (corresponding to $\phi = 1$). The curves correspond to different z values. At $\xi = 10$, the curves increase with decreasing z from $z = 1$ to $z = 0.1$ in steps of 0.1.

Fig. 4 The peculiarly normalised cross section for $\gamma^* q \to V q$, calculated numerically by successively iterating the BFKL kernel. The dotted line corresponds to two gluon exchange, the dashed line incorporates the corrections predicted by the first iteration (of the BFKL kernel), the solid line is the prediction after the second iteration and the diamonds are the predictions after the third iteration. The dash-dot line is the asymptotic result obtained by computing eq.(9) numerically. No resummation of the double logarithms has been performed. (a)$z = 0.05$; (b) $z = 0.35$.

Fig. 5 As in fig.4 except that the double logarithms have been resummed in the manner described in the text.

Fig. 6 As in fig.5, but for (a) $z = 0.2$; (b) $z = 0.5$; (c) $z = 0.8$.

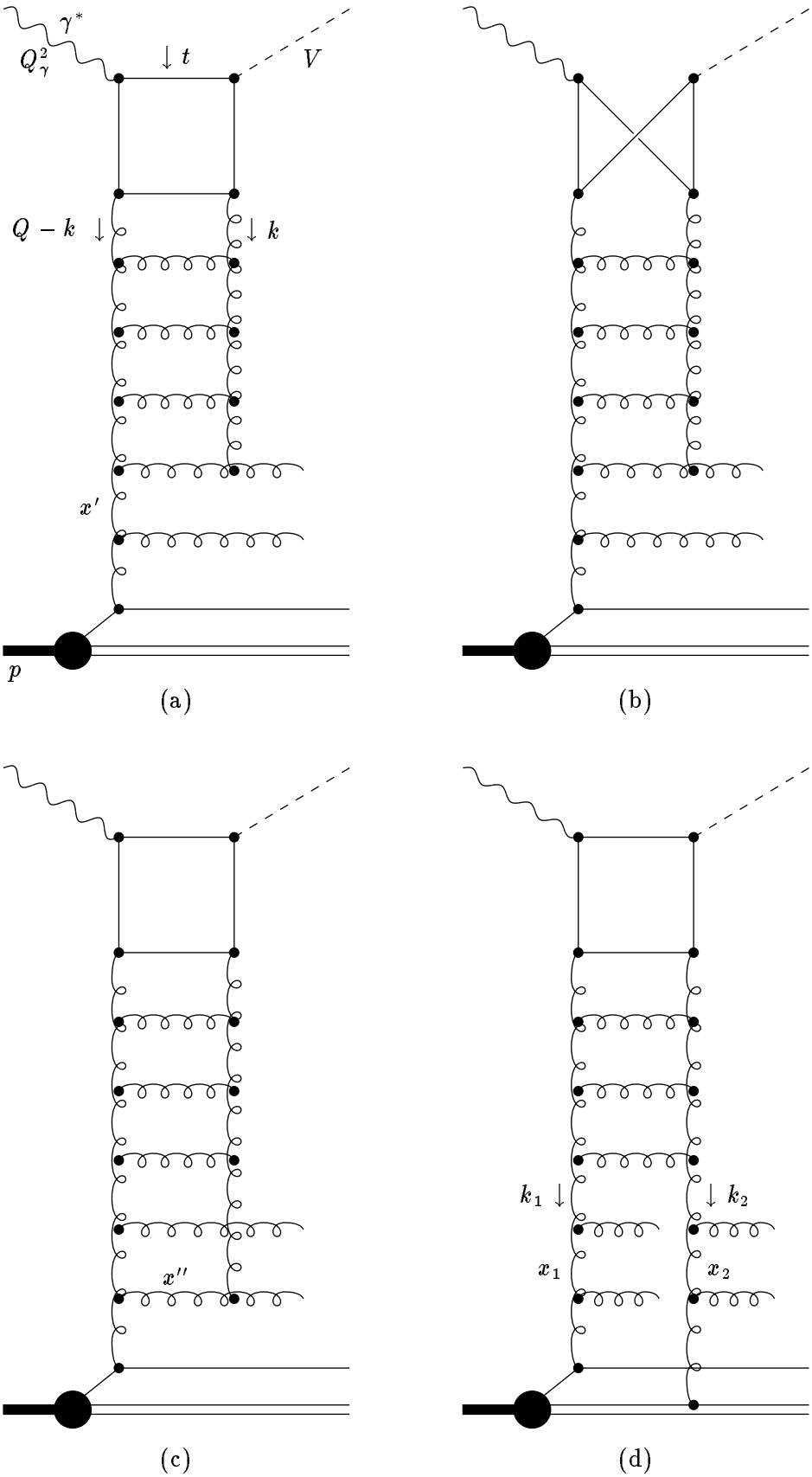
γ^*
Q_γ^2
$\downarrow t$
V
$Q-k$ $\downarrow$
$\downarrow k$
x'
p
(a)
(b)
x''
(c)
k_1 $\downarrow$
$\downarrow k_2$
x_1
x_2
(d)

Figure 1

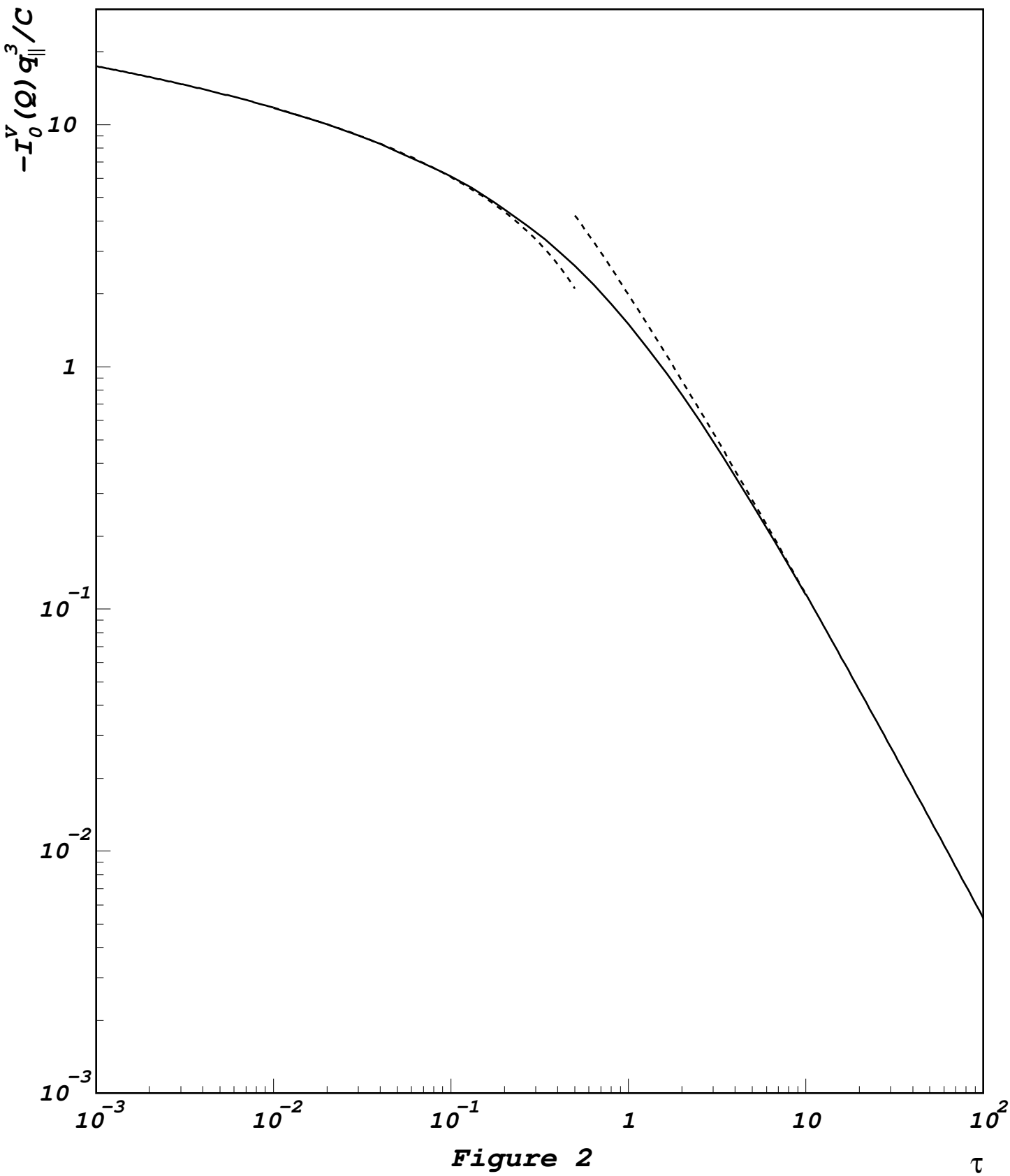

Figure 2

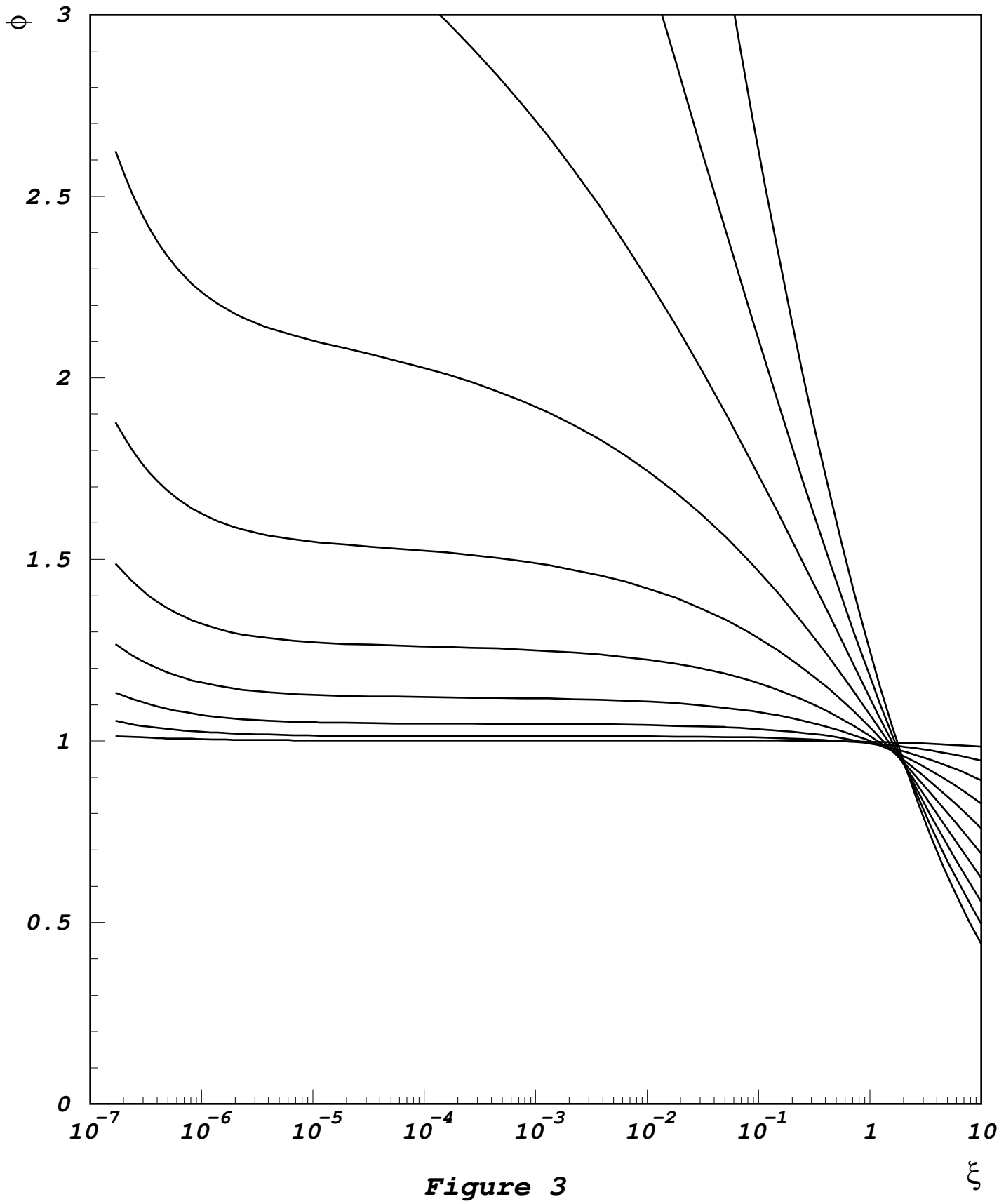

Figure 3

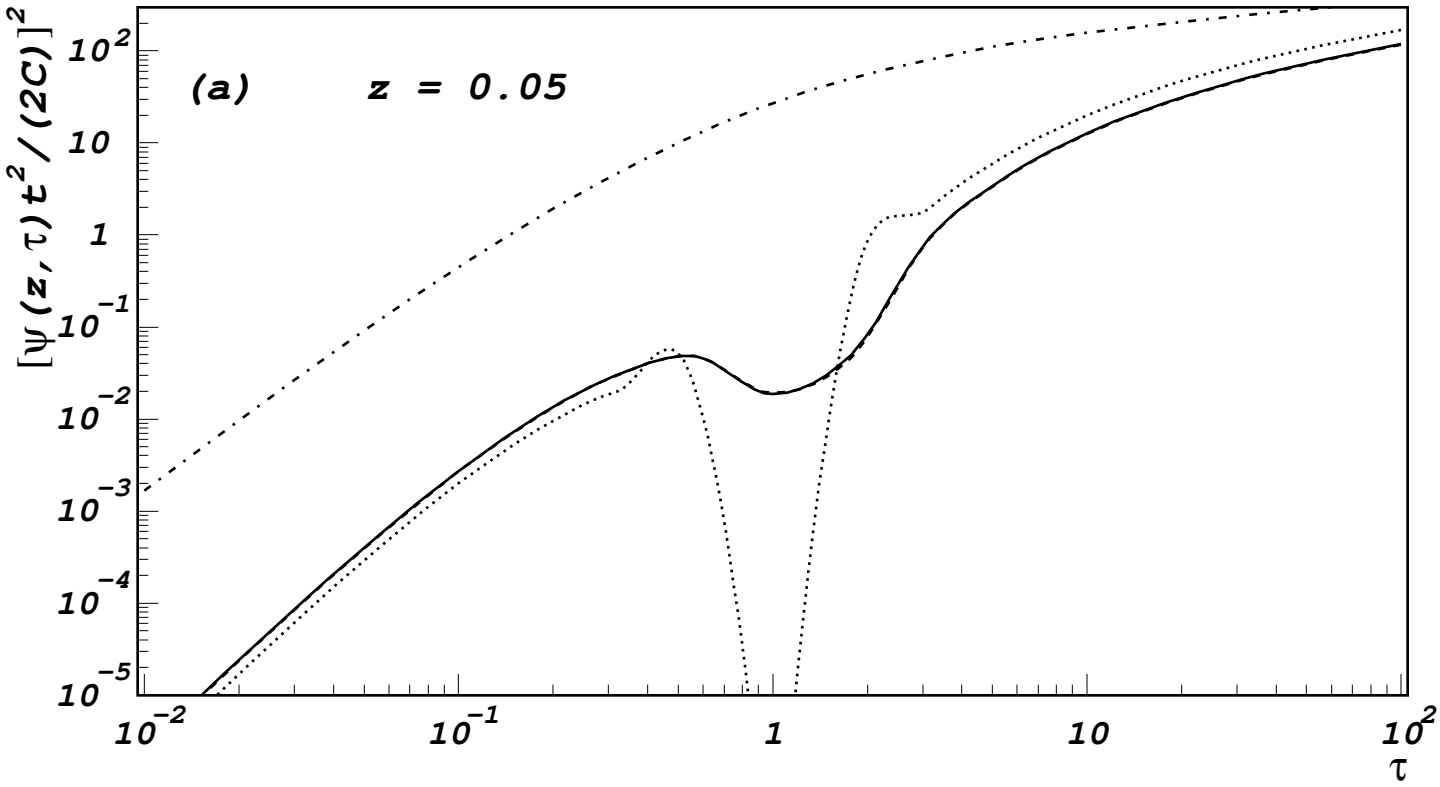
(a)
z = 0.05
$[\psi(z,\tau)t^2/(2C)]^2$
10^2
10
1
10^{-1}
10^{-2}
10^{-3}
10^{-4}
10^{-5}
10^{-2}
10^{-1}
1
10
10^2
τ

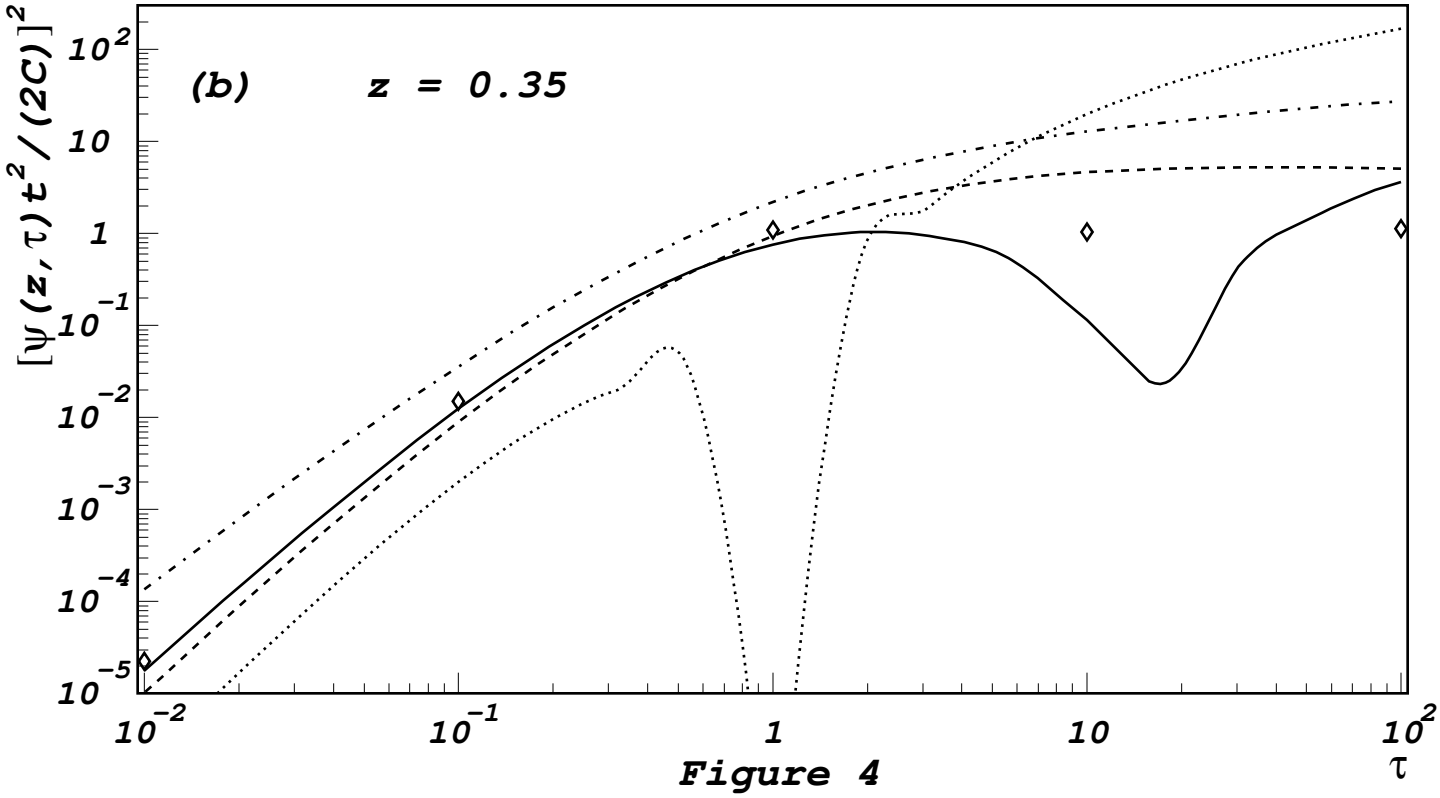
(b)
z = 0.35
$[\psi(z,\tau)t^2/(2C)]^2$
10^2
10
1
10^{-1}
10^{-2}
10^{-3}
10^{-4}
10^{-5}
10^{-2}
10^{-1}
1
10
10^2
τ

Figure 4

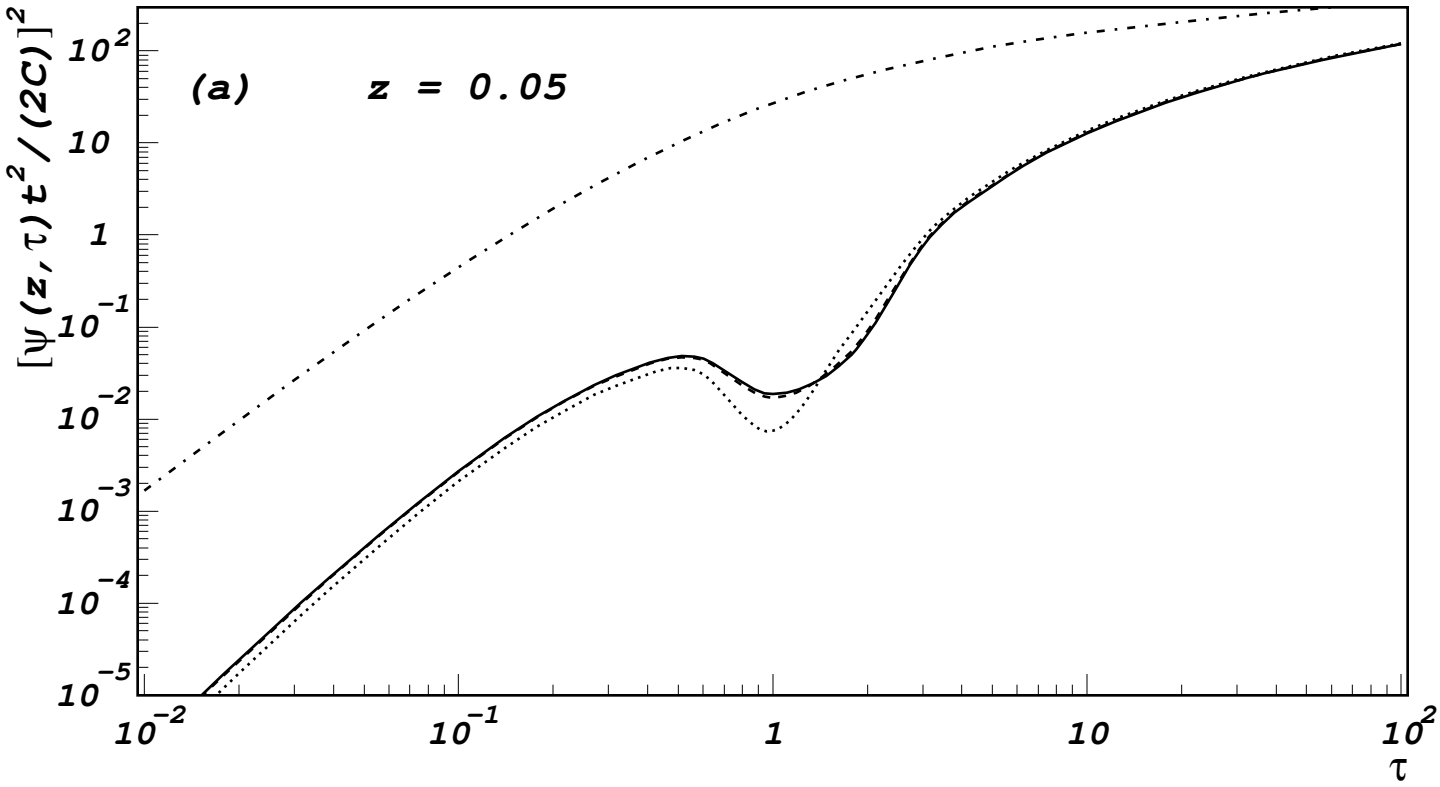
(a)
z = 0.05
$[\psi(z,\tau)t^2/(2C)]^2$
10^2
10
1
10^{-1}
10^{-2}
10^{-3}
10^{-4}
10^{-5}
10^{-2}
10^{-1}
1
10
10^2
τ

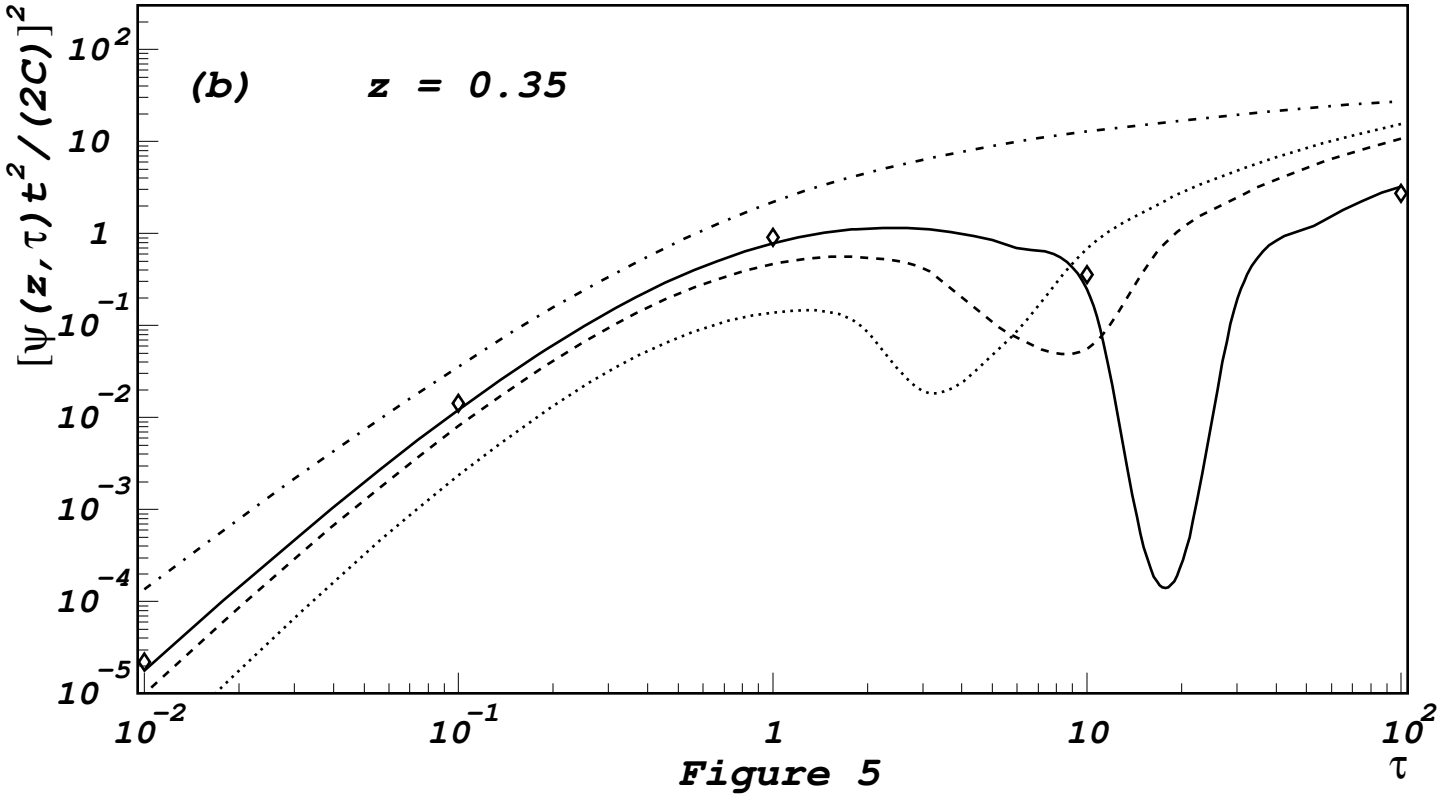
(b)
z = 0.35
$[\psi(z,\tau)t^2/(2C)]^2$
10^2
10
1
10^{-1}
10^{-2}
10^{-3}
10^{-4}
10^{-5}
10^{-2}
10^{-1}
1
10
10^2
τ

Figure 5

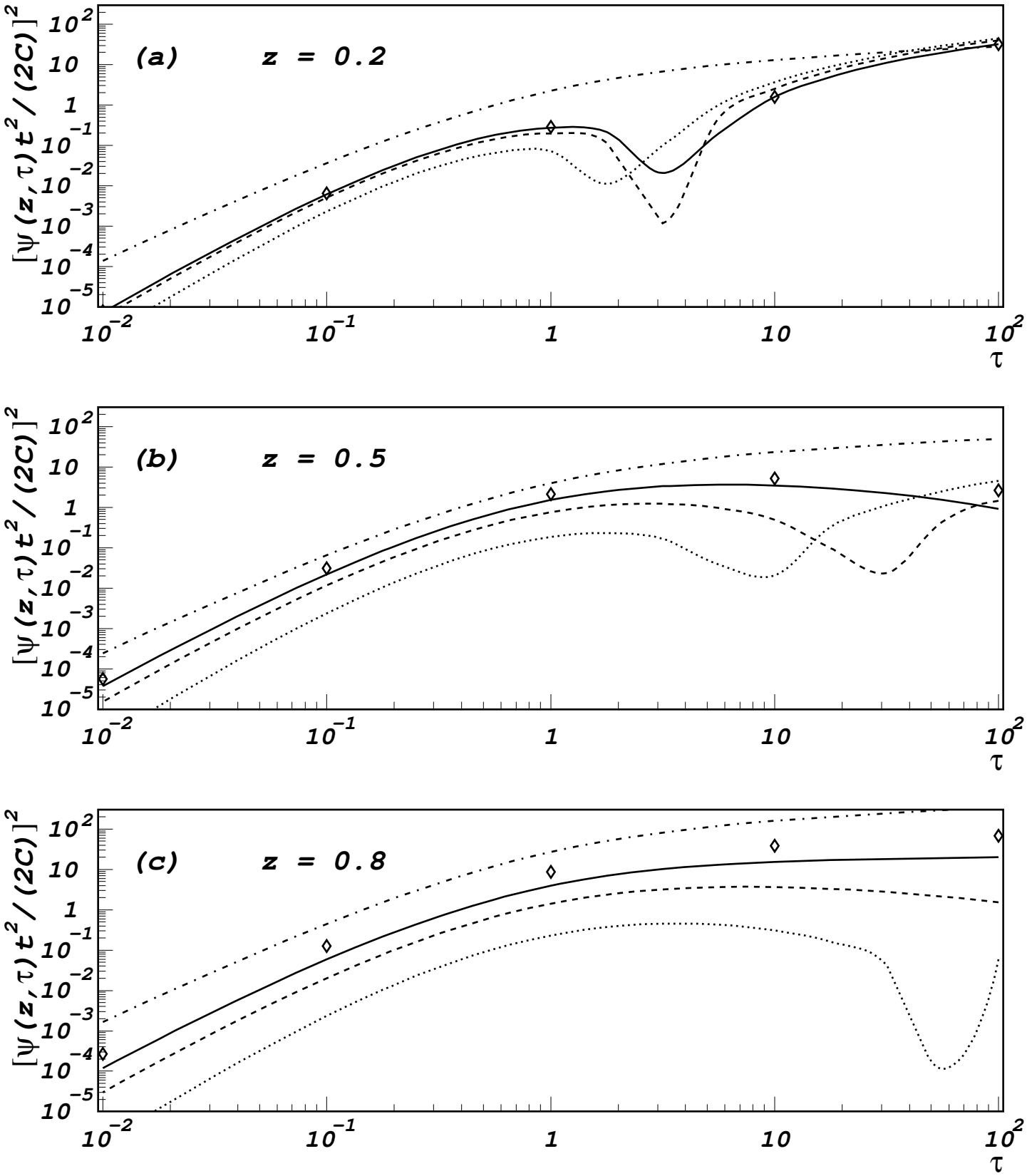

Figure 6